Channel Estimation for Mixed-Analog to Digital Converters Architecture in Massive MIMO Architecture Using Approximate Conjugate Gradient Pursuit Algorithm

Yaseen A. Mohammed[1], Anas L. Mahmood[2*]

Authors affiliations:
1) Department of Electronic and Communications Engineering, Al-Nahrain University, Baghdad-Iraq.
st.yaseen.aiman.mohammed@nahrainuniv.edu.iq

2*) Department of Electronic and Communications Engineering, Al-Nahrain University, Baghdad-Iraq.
anas.lateef.1@nahrainuniv.edu.iq

Paper History:

Received: 22nd July 2024

Revised: 3rd Dec. 2024

Accepted: 17th Dec. 2024

Abstract

Millimeter Wave (mmWave) Massive Multiple Input Multiple Out (MIMO) system is a key technology for future wireless transmission. The system's architecture can differ based on the type of Analog-to-Digital Converters (ADCs) used at the receiver, whether they are all low-resolution or a mix of different resolutions (Mixed-ADCs). Mixed-ADCs is a promising solution to achieve better performance than low-resolution ADC-only architectures by leveraging high-resolution ADCs to capture critical signal components while maintaining energy efficiency through low-resolution ADCs. In this paper, the problem of channel estimation for this system architecture is taken into consideration. A novel compressive-sensing based algorithm, that is called Approximate Conjugate Gradient Pursuit (ACGP), is proposed to estimate the channel coefficients. The performance of the proposed algorithm is investigated under varying system parameters, including different Signal-to-Noise Ratios (SNR), Radio Frequency (RF) chains, ADC resolutions, and numbers of observation frames. Matlab software was used to perform numerical simulations. The results demonstrated that mixed-ADCs architecture outperforms low resolutions only in performance. It was found that ACGP achieves lower Minimum Mean Squared Error (MMSE) compared to Orthogonal Matching Pursuit (OMP) and Least Square (LS), particularly in low SNR conditions showcasing its robustness and efficiency in signal reconstruction, achieving an average enhancement of 30% to 50% at moderate SNR levels. While OMP exhibited faster computation times under various number of observation frames, ACGP maintained stable computational performance, with a slight increase in computation time. For applications where accurate channel estimation is required under noisy environment, the proposed algorithm is an effective choice to meet such requirements.

Keywords: Massive MIMO, mmWave, Channel Estimation, 6G.

تخمين القناة للمعمارية المحولات التماثلية إلى الرقمية ذات الدقة المختلطة في نظام الهوائيات المتعددة الهائلة باستخدام خوارزمية الملاحقة التقريبية للاتجاه المترافق

ياسين ايمن محمد، انس لطيف محمود

الخلاصة:

نظام الهوائيات المتعددة الضخمة (Massive MIMO) بتقنية الموجات المليمترية (mmWave) يعتبر تقنية محورية لنقل البيانات لاسلكيًا في المستقبل. يمكن أن تختلف بنية النظام بناءً على المحولات التماثلي إلى الرقمية (ADCs)، سواء كانت هذه المحولات جميعها ذات دقة منخفضة أو مزيج من الدقات المختلفة. المحول التماثلي إلى الرقمي (ADC) ذو الدقة المختلطة هو حل واعد لتحقيق أداء أفضل من المعمارية ذات المحول التماثلي إلى الرقمي ذي الدقة المنخفضة فقط في اتصالات الموجات المليمترية (mmWave) بنظام الهوائيات المتعددة الضخمة (Massive MIMO). في هذه

NJES is an **open access Journal** with **ISSN 2521-9154** and **eISSN 2521-9162**

الورقة، يتم تناول مشكلة تخمين معاملات القناة لهذا النظام ذو معمارية الدقة المختلطة. يتم اقتراح خوارزمية جديدة تعتمد على الاستشعار الانضغاطي(compressive-sensing)، تسمى (Approximate Conjugate Gradient Pursuit (ACGP، لتخمين معاملات القناة. تم التحقيق في أداء الخوارزمية المقترحة تحت ظروف نظام مختلفة، بما في ذلك نسب الإشارة إلى الضوضاء (SNR) المختلفة، سلاسل التردد اللاسلكي (RF)، دقة المحولات التماثلية إلى الرقمية (ADC)، وعدد الإشارات التي يتم رصدها. أظهرت النتائج الرقمية أن معمارية الـ ADC ذات الدقة المختلطة تتفوق في الأداء على المعمارية ذات الدقة المنخفضة فقط. ووجد أن خوارزمية ACGP تحقق فرق متوسط أدنى (MMSE) مقارنة بخوارزمية (OMP) وخوارزمية (LS)، خاصة في ظروف الـ SNR المنخفضة، مما يظهر قوتها وكفاءتها في تخمين الإشارة. بينما أظهرت خوارزمية OMP أوقات حساب أسرع تحت عدد مختلف من الإشارات التي تم رصدها، حافظت خوارزمية ACGP على أداء متوازن مع زيادة طفيفة فقط في وقت التخمين. للتطبيقات التي تتطلب تقدير قناة دقيق في ظروف ضوضاء عالية، فإن الخوارزمية المقترحة تعتبر اختيارًا فعالًا لتلبية هذه المتطلبات.

1. Introduction

The Massive multiple-input multiple output (MIMO) Millimeter wave (mmWave) wireless communication is a primary enabler for sixth generation (6G) wireless transmissions [1], [2]. The system architecture promises to efficiently exploit the available bandwidth at millimeter wave's spectrum (20-300 GHz) [3], [4], [5]. The main concern in mmWave is the significant path loss incurred at a much higher rate than the lower frequency bands. Nevertheless, large scale antenna arrays (Massive) utilizing beamforming can improve coverage and reduce interference and power consumption [6]. The use of the mmWave frequency bands increase the requirements of the hardware architecture as high-resolution analog-to-digital converters (ADCs) are cost-ineffective. One solution that has been proposed in the literature [6], [7] is to use hybrid precoding structure, i.e., reducing the number of radio frequency (RF) chains and eventually, using a smaller number of ADCs. An alternative solution is to use low resolution ADCs only, which immensely reduce cost and power requirements at the expense of the severe quantization noise.

Over the last decade, there has been a huge number of channel estimation algorithms, tackling the channel estimation problem in Massive MIMO mmWave communications. The channel estimation can be categorized according to the architecture of the system. In [8], [9], high resolution ADCs were used in the system architecture whereas in [5], [10], fully-digital architecture was implemented with low resolution ADCs. Implementing fully-digital structure, i.e., each antenna is connected to a separate RF chain, is limited by cost and complexity when the number of antennas rises to massive. On the other hand, while using low resolution ADCs is a fit for fully-digital structure, it causes a severe quantization noise problem in the hybrid precoding structure. Using high and low resolutions ADCs could alleviate the quantization noise severity and enhance the beamforming performance [11], [12]. This mixed-ADC architecture has been proposed as cost-effective and power efficient since the majority of antennas are connected to low resolution ADCs while the minority are connected to high resolution ADCs.

The mmWave channel has few non-zero elements, i.e., the channel matrix happens to be very sparse. As a result, the channel estimation problem is naturally solved using compressed sensing technology [13], [14], [15], [16]. In [13] and [14], Orthogonal matching Pursuit was proposed to recover the mmWave Massive MIMO channel matrix. The authors in [16], [17] proposed to use time and frequency domain methods for wideband channel recovery. In [18], the authors used a neural network iterative-weighting and learning based scheme to estimate the angles of arrival/departure of the array response vectors. In [19], CSI sensing and recovery network were combined to have a better real-time CSI feedback architecture. In [20], iterative algorithms (Approximate Message Passing, AMP) and Deep Learning (DL) schemes were combined to develop a learned denoising based AMP, that is called, LDAMP. Lastly, to reduce the overall system overhear, a DL based approach was proposed in [21].

There have been numerous studies on the performance of the mixed-ADCs architecture, whereas the channel estimation problem has not been tackled sufficiently yet. In this paper, we propose a compressed sensing algorithm named Approximate Conjugate Gradient Pursuit (ACGP), designed to reduce complexity while maintaining robust performance. Unlike traditional algorithms such as Orthogonal Matching Pursuit (OMP) and Least Squares (LS), ACGP leverages approximated conjugate and gradient directions, which enhances its efficiency in estimating sparse mmWave channels under mixed-ADC architectures. This facilitates for improved channel estimation, particularly in low-SNR environments, while significantly reducing computational overhead compared to existing methods. The algorithm's performance is benchmarked against OMP [1] and LS to highlight its advantages.

The main contributions of this paper are summarized as follows:

- Proposal of ACGP Algorithm: Introduces a novel compressed sensing algorithm, Approximate Conjugate Gradient Pursuit (ACGP), for channel estimation in mmWave massive MIMO systems with mixed-ADC architectures.

NJES is an **open access Journal** with **ISSN 2521-9154** and **eISSN 2521-9162**

- Enhanced Estimation Efficiency: Leverages approximated conjugate and gradient directions to achieve accurate sparse channel estimation, particularly under challenging low-SNR conditions, with reduced computational complexity.
- Extensive Performance Analysis: Evaluates ACGP under various system parameters, such as SNR levels, RF chains, ADC resolutions, and observation frames, demonstrating its robustness across diverse scenarios.
- Superior to Baseline Methods: Benchmarks ACGP against traditional algorithms like OMP and LS, showing significantly improved MMSE performance and reduced computational overhead.
- Mixed-ADC Architecture Benefits: Highlights the effectiveness of mixed-ADC architectures over low-resolution ADC-only systems, offering improved channel estimation accuracy while preserving energy efficiency.

The rest of the paper is organized as follows. Section 2 illustrates the proposed architecture of the Massive MIMO system. Section 3 delves through the steps of the proposed algorithm. Section 4 provides the numerical and simulation analysis of the proposed system and algorithm. Finally, the research is concluded in section 5.

2. System Model

A mmWave Massive MIMO communication system is considered, provided with a hybrid beamforming architecture and mixed-ADCs similar to the system shown in Fig.1. The number of antennas utilized for the BS and MS are N_{Bt} and N_{Mr}, respectively. L denotes the number of RF chains used at both ends. The data streams' number is denoted by N_s and it is assumed to be equal to L.

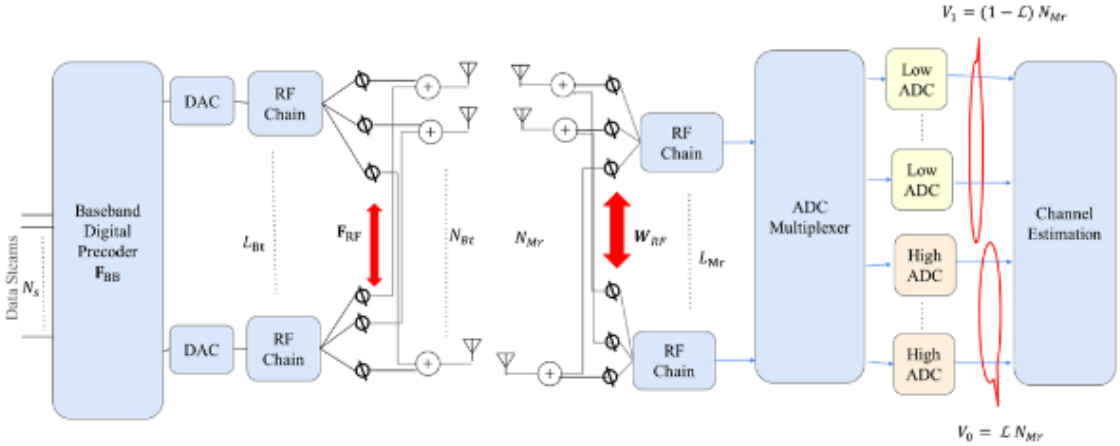

Figure (1): Single user Massive MIMO with mixed-ADCs architecture

The BS is provided with $L \times N_s$ baseband precoder $\mathbf{F}_{\mathrm{BB}}$ and is succeeded by $N_{Bt} \times L$ RF precoder $\mathbf{F}_{\mathrm{RF}}$. The signal at the m^{th} time after the precoder can be written as [1]:

$$\mathbf{x}_m = \mathbf{F}_{\mathrm{m}}\, \mathbf{s}_m \qquad \dots (1)$$

Where $\mathbf{F} = \mathbf{F}_{\mathrm{RF}}\, \mathbf{F}_{\mathrm{BB}}$, and $\mathbf{s}_m$ denotes the transmitted symbols at the m^{th} time. For the purpose of normalization, the vector $\mathbf{s}$ should de be implemented such that $\mathrm{E}\,[\mathbf{s}\mathbf{s}^{\boldsymbol{H}}] = (\frac{1}{N_s})\boldsymbol{I}_{N_s}$. The received vector at the m^{th} time can be written in the form [1]:

$$\mathbf{r}_m = \sqrt{P}\,\mathbf{H}\,\mathbf{F}_m\,\mathbf{s}_m + \mathbf{n}_m \qquad \dots (2)$$

Where the mmWave channel is $\mathbf{H}$ with $N_{Mr} \times N_{Bt}$ dimensions, and $\mathbf{n}_m \sim \mathcal{N}(0, \sigma^2\, \mathbf{I}_{N_{Mr}})$ denotes the additive white Gaussian noise. P is the transmission power The combiner $\mathbf{W}_{\mathrm{m}}$ at the MS is found by the product of the RF and BS combiners $\mathbf{W}_{\mathrm{RF}}$ and $\mathbf{W}_{\mathrm{BB}}$ to have the below received signal [1]:

$$\mathbf{y}_m = \sqrt{\mathrm{P}}\,\mathbf{W}_{\mathrm{m}}^{\mathrm{H}}\,\mathbf{H}\,\mathbf{F}_{\mathrm{m}}\,\mathbf{s}_m + \mathbf{W}_{\mathrm{m}}^{\mathrm{H}}\,\mathbf{n}_m \qquad \dots (3)$$

A mixed-ADCs system architecture is considered at the MS side. The MS is equipped with high- and low-resolution ADCs where the majority of the antennas are connected to low resolution ADCs whereas the minority are connected to high resolution ADCs. It is supposed that $V_0 = \mathcal{L}\,N_{Mr}$ represents the number of antennas which are connected to the high-resolution ADCs and $V_1 = (1-\mathcal{L})\,N_{Mr}$ represents the number of antennas connected to the low-resolution ADCs, resembling the majority of antennas. $\mathcal{L}$ can be taken as a percentage of the total number of antennas. The overall received vector $\mathbf{Y}$ can be written as [1]:

$$\mathbf{Y} = \begin{bmatrix}\mathbf{Y}_0 \\ \breve{\mathbf{Y}}_1\end{bmatrix} = \begin{bmatrix}\mathbf{Y}_0 \\ \mathcal{Q}(\mathbf{Y}_1)\end{bmatrix}$$

$$= [\boldsymbol{y}[1], \dots, \boldsymbol{y}[V_0], \mathcal{Q}(\boldsymbol{y}[V_0+1]), \dots, \mathcal{Q}(\boldsymbol{y}[V_1])]^T$$

It is assumed that the high-resolution ADCs has negligible quantization noise as such low-resolution ADCs quantization noise contribution are taken into account only. The mmWave channel is modeled as geometric and a limited number of K scatterers is assumed, where each scatterer is proposed to contribute to a single propagation path between the BS and the MS. Hence, the u^{th} tap channel $\mathbf{H}_u$ can be determined as [23]:

$$\mathbf{H}_u = \sqrt{\frac{N_{Mr} N_{Bt}}{\rho}} \sum_{k=1}^{K} \alpha_k \, \mathbf{a}_{MS}(\theta_k) \, \mathbf{a}_{BS}{}^{H}(\phi_k) \quad \dots (4)$$

Where the average path-loss is denoted by ρ. And the complex gain of the k^{th} path is referred to as α_k, it is assumed to have a Rayleigh distribution, i.e., $\alpha_k \sim \mathcal{N}(0, \overline{P_R})$, k = 1,2, ..., K with the average power gain $\overline{P_R}$. θ_k and ϕ_k represent the azimuth angles of arrival and departure, respectively. They are assumed to be uniformly distributed between 0 and 2π. Lastly, $\mathbf{a}_{MS}(\theta_k)$ and $\mathbf{a}_{BS}(\phi_k)$ are the array response vectors at the BS and MS, respectively. The array response vector at the MS can be formulated as [23]:

$$\mathbf{a}_{MS}(\theta_k) = \sqrt{\frac{1}{N_{Mr}}} \begin{bmatrix} 1, e^{j\left(\frac{2\pi}{\lambda}\right) dsin(\theta_k)}, \dots . \\ \dots, e^{j(N_{Mr}-1)\left(\frac{2\pi}{\lambda}\right) dsin(\theta_k)} \end{bmatrix}^T \quad \dots (5)$$

Where λ refers to the wavelength, and d denotes the antenna elements spacing. The array response vector at the BS can be determined in the same manner as in eq. (5). In this paper, it is assumed that any prior knowledge of the channel is not available. The channel can be reformulated as [1], [24]:

$$\mathbf{H}_u = \mathbf{A}_R \, \mathrm{diag}(\boldsymbol{\alpha}) \, \mathbf{A}_T^H \quad \dots (6)$$

Where

$$\boldsymbol{\alpha} = \sqrt{\frac{N_{Mr} N_{Bt}}{\rho}} \, [\alpha_1, \alpha_2, \dots \dots, \alpha_K]$$

$$\mathbf{A}_T = [a_T(\phi_1), a_T(\phi_2), \dots ., a_T(\phi_K)]$$

$$\mathbf{A}_R = [a_R(\theta_1), a_R(\theta_2), \dots \dots, a_R(\theta_K)]$$

Combining all the narrowband channels of all clusters leads to the wideband channel model that can be simplified as [8]:

$$\mathbf{H} = \sum_{u=1}^{N_c} \mathbf{H}_u \quad \dots (7)$$

Where N_c refers to the number of clusters.

The received matrix ($\mathbf{y}_m$) before quantization is formulated as [1], [25]:

$$\begin{aligned} \mathbf{y}_m &= \sqrt{P} \, \mathbf{W}_m^H \, \mathbf{H} \, \mathbf{F}_m \, \mathbf{s}_m + \mathbf{W}_m^H \, \mathbf{n}_m \\ &= \sqrt{P} \left(\mathbf{S}_m^T \, \mathbf{F}_m^T \otimes \mathbf{W}_T^H \right) \mathrm{vec}(\mathbf{H}) + \mathbf{N}_m \end{aligned} \quad \dots (8)$$

Where $\mathbf{N}_m = \mathbf{W}_m^H \, \mathbf{n}_m$. As derived in [1], [25], the overall received signal consisting of all M frames can be written in the form [1], [25]:

$$\begin{aligned} \mathbf{Y} &= \sqrt{P} \, \boldsymbol{\Psi} \, \mathbf{z} + \mathbf{N} \\ \mathbf{Y} &= \sqrt{P} \, \boldsymbol{\phi} \, \mathbf{A}_D \, \mathbf{z} + \mathbf{N} \end{aligned} \quad \dots (9)$$

Where $\mathbf{y}$ are the obtainable observations, $\boldsymbol{\Psi}$ is the sensing matrix ($\boldsymbol{\Psi} = \boldsymbol{\phi} \, \mathbf{A}_D$), and $\boldsymbol{\phi}_m$ is the measurement matrix of the m^{th} time frame ($\boldsymbol{\phi}_m = \mathbf{S}_m^T \, \mathbf{F}_m^T \otimes \mathbf{W}_T^H$). $\mathbf{A}_D$ is a dictionary matrix or sparse basis matrix whose elements can be determined by utilizing all the AOA/AOD's possible values [1], [25]. The paths' gains of the quantized directions is denoted by the vector $\boldsymbol{z}$. The mmWave Massive MIMO channel is very sparse due to the lack of line-of-sight components. The sensing matrix $\boldsymbol{\Psi}$ is used to predict the sequence $\mathbf{z}$. Then, by utilizing the basis matrix $\boldsymbol{A}_D$, we can recover the channel matrix.

3. Approximate Conjugate Gradient Pursuit Algorithm (ACGP)

To contextualize the performance of the proposed Approximate Conjugate Gradient Pursuit (ACGP) algorithm, it is essential to compare it with established baseline methods such as Orthogonal Matching Pursuit (OMP) and Least Squares (LS) algorithms [1]. These algorithms represent standard approaches in compressive sensing and channel estimation, each with its unique strengths and limitations.

OMP algorithm is a traditional greedy algorithm widely used in compressive sensing for signal reconstruction. It iteratively selects the atom with the highest correlation to the current residual, leveraging the signal's sparsity. By orthogonalizing the selected atoms during execution, OMP minimizes the required number of measurements and iterations, making it computationally efficient.

LS algorithm, on the other hand, relies on straightforward mathematical operations such as matrix inversion and multiplication. This simplicity makes LS easy to implement with fewer parameters. However, LS does not account for the effects of noise, leading to inaccuracies in channel estimation, particularly in low signal-to-noise ratio (SNR) conditions.

In this paper, we propose using a different implementation of Orthogonal Matching Pursuits (OMP). The computational complexity of OMP comes from using the pseudo-inverse operation in each iteration of the algorithm to calculate the recovered vector $\mathbf{z}$. This operation is time consuming and requires excessive memory, hence, efficient implementation should be developed. The first efficient implementation is using QR factorization while the second one, which is considered in this paper, is using directional updates. The latter one has similar computational complexity to the QR factorization but if offers: better stability, less storage requirements, and a smaller number of multiplications. However, while the directional updates provide computational efficiency, the approximations involved in this approach may lead to performance deficiencies in certain scenarios. For example, in cases where the sensing matrix columns exhibit high correlation, the index selection process may be less reliable, affecting the quality of the reconstruction. Additionally, when the number of iterations is limited, the algorithm may not fully converge, leading to suboptimal channel estimation.

The algorithm starts by firstly defining $\boldsymbol{\Psi}$ sensing matrix, which maps the high-dimensional sparse signal

to a lower-dimensional observed signal while preserving sufficient information for reconstruction. It also defines the observation vector $\mathbf{y}$, the length of the recovered vector $\mathbf{z}$, and the number of iterations **maxi**. Then, the algorithm initializes the residual vector $\boldsymbol{r}^{\mathbf{0}}$, which represents the difference between the observed signal and the reconstructed signal, the recovered vector $\mathbf{z}^{\mathbf{0}}$, and the indexing variable $\boldsymbol{\Gamma}^{0}$. The algorithm, then, finds the correlation between the Hermitian of sensing matrix $\boldsymbol{\Psi}^{\mathrm{H}}$ and the residual $\boldsymbol{r}^{\mathbf{n-1}}$. Next, the algorithm searches for the index referring to the maximum correlation, performs the union of the previous indexing symbol $\boldsymbol{\Gamma}^{n-1}$, and assigns this value to $\boldsymbol{\Gamma}^{n}$. After that, the direction $\boldsymbol{d}_{\boldsymbol{\Gamma}^{n}}^{n}$ is updated for all n, (except when n=1, the first direction $\boldsymbol{d}_{\boldsymbol{\Gamma}^{1}}^{1}$ = 1) by combining the previous update direction ($b_1\ \boldsymbol{d}_{\boldsymbol{\Gamma}^{n}}^{n-1}$) and the current gradient direction ($\boldsymbol{g}_{\boldsymbol{\Gamma}^{n}}$), which indicates the direction of the steepest descent in the error space. This direction helps adjust the reconstructed signal in each iteration by refining the estimate toward a more accurate solution. The optimal step-size a^n is, then, calculated and multiplied by the new direction to find the updated values of the vector $\boldsymbol{z}^{\boldsymbol{n}}$. The algorithm runs through the steps until the maximum number of iterations is reached. Finally, the vector $\mathbf{z}$ is utilized to estimate the channel matrix $\mathbf{H}$ in a vectorized form h. The algorithm is summarized in Algorithm 1.

Following the algorithm steps, the computational complexity of the proposed ACGP algorithm can be upper bounded by $\mathcal{O}(K_s N_{\boldsymbol{\Psi}} M_{\boldsymbol{\Psi}})$, where K_s is the sparsity level, $N_{\boldsymbol{\Psi}}$ is the number of columns in the sensing matrix, and $M_{\boldsymbol{\Psi}}$ is the number of rows. In comparison, the LS algorithm has a complexity of $\mathcal{O}(N_{\boldsymbol{\Psi}}^3)+\mathcal{O}(M_{\boldsymbol{\Psi}} N_{\boldsymbol{\Psi}}^2)$, while the OMP algorithm exhibits a complexity of $\mathcal{O}(K_s^3) + \mathcal{O}(M_{\boldsymbol{\Psi}} K_s^2)+ \mathcal{O}(K_s N_{\boldsymbol{\Psi}} M_{\boldsymbol{\Psi}})$. These results highlight that the ACGP algorithm incurs significantly lower computational overhead, particularly in terms of the number of operations required, making it more efficient than both LS and OMP in practical implementations.

Algorithm 1: Approximate Conjugate Gradient Pursuit algorithm (ACGP)

Input: The sensing matrix is $\boldsymbol{\Psi}$, observations vector $\mathbf{y}$, the length of the approximated vector $\mathbf{z}$, and the number of iterations (**maxi**)

1. Initialize: $\boldsymbol{r}^{\mathbf{0}} = \boldsymbol{y}, \mathbf{z}^{\mathbf{0}} = 0, \boldsymbol{\Gamma}^{0} = \emptyset$
2. for n = 1; $n := n + 1$ till maxi
3. $\boldsymbol{g}^{n} = \boldsymbol{\Psi}^{\mathrm{H}}\, \boldsymbol{r}^{n-1}$
4. $\boldsymbol{\Gamma}^{n} = \boldsymbol{\Gamma}^{n-1} \cup \{\arg_i \max|\boldsymbol{g}_i|\}$
5. if n = 1
   - $\boldsymbol{d}_{\boldsymbol{\Gamma}^{1}}^{1}$ = 1
6. if $n \neq 1$
   - $b_1 = -\boldsymbol{c}^{n-1^*}\boldsymbol{\Psi}_{\boldsymbol{\Gamma}^{n}}\boldsymbol{g}_{\boldsymbol{\Gamma}^{n}} / (\boldsymbol{c}^{n-1^*}\, \boldsymbol{c}^{n-1})$
     Where $\boldsymbol{c}^{n} = \boldsymbol{\Psi}_{\boldsymbol{\Gamma}^{n}}\, \boldsymbol{d}_{\boldsymbol{\Gamma}^{n}}^{n}$
   - $\boldsymbol{d}_{\boldsymbol{\Gamma}^{n}}^{n} = \boldsymbol{g}_{\boldsymbol{\Gamma}^{n}} - b_1\, \boldsymbol{d}_{\boldsymbol{\Gamma}^{n}}^{n-1}$
7. $a^n = \boldsymbol{r}^{n^*}\boldsymbol{c}^{n} / (\boldsymbol{c}^{n^*}\, \boldsymbol{c}^{n})$
8. $\boldsymbol{z}^{\boldsymbol{n}} := \boldsymbol{z}_{\boldsymbol{\Gamma}^{n}}^{n} = \boldsymbol{z}_{\boldsymbol{\Gamma}^{n}}^{n-1} + a^n\, \boldsymbol{d}_{\boldsymbol{\Gamma}^{n}}^{n}$
9. $\boldsymbol{r}^{n} = \boldsymbol{r}^{n-1} - a^n\, \boldsymbol{c}^{n}$
10. end for
11. $\boldsymbol{z} = \boldsymbol{z}^{\boldsymbol{n}}$
12. $\mathbf{h} = \mathbf{A}_{\mathrm{D}}\, \mathbf{z}$
13. Output: $\mathbf{h}$

4. Numerical Results

In this section, we compare the performance of the proposed algorithm with OMP and LS algorithms presented in [1] in terms of the achieved Minimum Mean Squared Error (MMSE). The system parameters are as follows: $L_{\mathrm{Bt}} = N_s = L_{\mathrm{Mr}} = 4$, $N_{Mr} = 16$, $N_c = 4$, $N_{Bt} = 32, K = 2$ (number of paths in each cluster), $N = 16$ symbols per frame, $M = 80$ number of observations or frames, $\mathcal{L}$ = 0.2. We will refer to any change of parameters as proceeded in this section.

Fig.2 depicts the performance comparison of the proposed algorithm (ACGP) with OMP for different radio frequency (RF) chains in terms of (MMSE) across varying Signal-to-Noise Ratios (SNR). The results show how the algorithms behave under different noise conditions. Each line represents a specific algorithm and RF combination: OMP with RF=1 (green triangles), ACGP with RF=1 (purple triangles), OMP with RF=2 (blue circles), ACGP with RF=2 (yellow circles), OMP with RF=4 (black dashed line with triangles), and ACGP with RF=4 (pink diamonds). As SNR increases, MMSE decreases for all algorithms, indicating improved estimation accuracy. Notably, ACGP with higher RFs (RF=4, RF=2) consistently achieves lower MMSE compared to OMP, especially at lower SNRs, depicting its robustness and superior performance in noisy environments.

A performance comparison is presented in terms of MMSE as a function of SNR for different ADC resolutions is illustrated in Fig.3. The algorithms compared are LS, OMP, and ACGP, each evaluated with 1-bit, 2-bit, 3-bit, and 4-bit ADCs. The plot indicates that, across all ADC resolutions, MMSE decreases as SNR increases, highlighting improved estimation accuracy at higher SNR levels. As it can be observed, ACGP consistently outperforms both OMP and LS across different ADC resolutions. The MMSE values for higher-resolution ADCs (4-bit) are significantly lower compared to those for 1-bit ADCs, depicting the advantage of higher ADC resolution in reducing estimation error. The results underscore the robustness of ACGP, especially with increased ADC resolution, in achieving lower MMSE, thus providing more accurate signal reconstruction under various noise conditions.

Fig.4 shows a comparing between mixed-ADCs architecture and low resolutions only architecture. The total number of high-resolution ADCs is assumed to be 13 since the percentage is $\mathcal{L}$ = 0.2. It can be observed that the impact of the proposed architecture is considerable. All algorithms show an enhancement in performance with the mixed resolution architecture. ACGP marks a better performance than OMP and LS, achieving lower MMSE for the whole SNR ranging from -10 to 10.

The impact of ADC resolution (in bits) on the performance of OMP and ACGP algorithms is demonstrated in Fig.5. The results indicate that for both algorithms, increasing the number of bits results

in a significant reduction in MMSE, especially when changing from 1-bit to 4-bit ADCs. At 0 dB SNR, ACGP consistently outperforms OMP, achieving lower MMSE across all bit resolutions. Similarly, at 10 dB SNR, both algorithms exhibit improved performance with increased ADC resolution, but ACGP again demonstrates superior accuracy compared to OMP until the resolution becomes 3 bits. The curves show negligible returns beyond 4 bits, where the reduction in MMSE becomes less promising. This indicates that while higher bit resolutions enhance performance, the most gains in essence are achieved within the 1-bit to 4-bit range, particularly for ACGP under both SNR conditions.

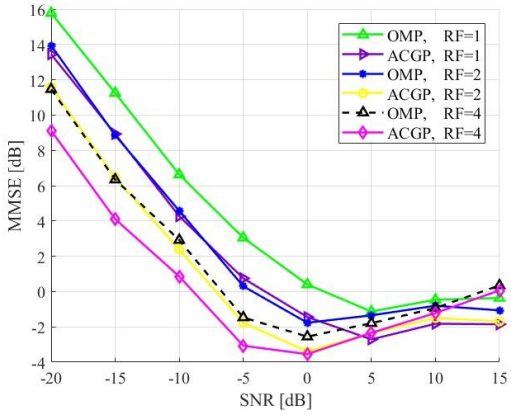

Figure (2): The MMSE of the proposed algorithm as compared with OMP for different RF chains

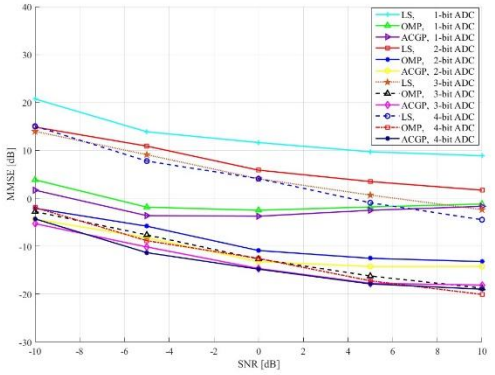

Figure (3): The algorithms achievable MMSE for different ADC resolutions

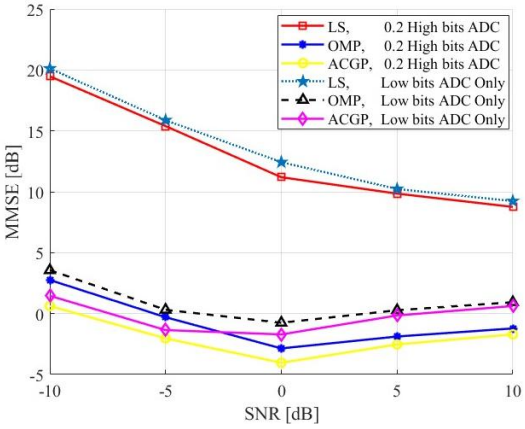

Figure (4): Performance comparison between mixed-ADCs and low resolutions ADCs only

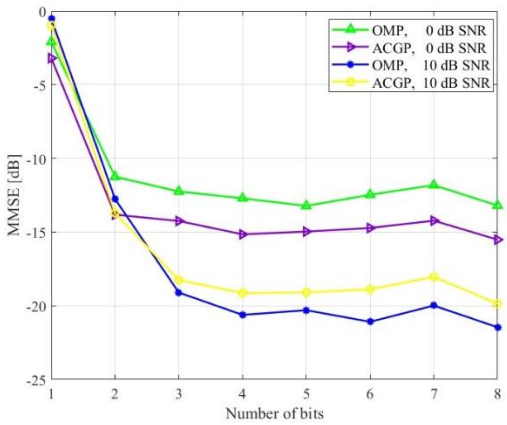

Figure (5): Performance comparison of the mixed-ADCs for different number of low resolutions ADCs bits

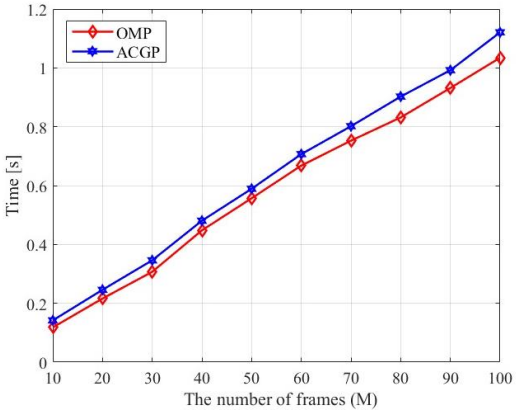

Figure (6): Computation time comparison for different number of frames (M)

Finally, Fig.6 shows a comparison in computation time of ACGP and OMP for different numbers of frames (M). It is clearly noticed that although OMP seems to be more efficient in processing, as for different number of observation frames (M), ACGP depicts a stable and almost constant difference in time. Despite OMP's faster computation times, ACGP offers significant advantages in terms of accuracy and robustness, particularly in noisy environments.

5. Conclusion

In this paper, the channel estimation problem for mmWave Massive MIMO with mixed-ADCs is studied. A compressed-sensing based algorithm is proposed and its performance is evaluated. Simulation results showed that mixed-ADC architectures significantly outperform low-resolution systems, with ACGP yielding lower Minimum Mean Squared Error (MMSE) than Orthogonal Matching Pursuit (OMP) and Least Squares (LS), particularly under low SNR conditions, achieving an average performance improvement of 30% to 50% at moderate SNR levels. The improved channel estimation accuracy provided by ACGP has broader implications for mmWave Massive MIMO systems. By delivering more reliable channel estimates, ACGP enables more effective beamforming and resource allocation, which are critical for enhancing overall system capacity, spectral efficiency, and energy efficiency. Although ACGP incurred a slight increase in computation time, it is considered less complex computation- and storage-

wise. It is also consistent accuracy and robustness make it efficient in massive MIMO systems. Future work could focus on further optimizations of ACGP to reduce computation time while preserving its high performance. One potential approach involves leveraging parallel processing techniques to expedite computations, particularly for large-scale systems. Incorporating machine learning techniques, such as deep neural networks, could also enhance the initialization phase or guide the selection of gradient directions, thereby improving both accuracy and efficiency.

References

[1] R. Zhang, L. Yang, M. Tang, W. Tan, and J. Zhao, "Channel Estimation for mmWave Massive MIMO Systems with Mixed-ADC Architecture," IEEE Open Journal of the Communications Society, vol. 4, pp. 606–613, 2023, doi: 10.1109/OJCOMS.2023.3242668.

[2] H. Wang, P. Xiao, and X. Li, "Channel Parameter Estimation of mmWave MIMO System in Urban Traffic Scene: A Training Channel-Based Method," IEEE Transactions on Intelligent Transportation Systems, vol. 25, no. 1, pp. 754–762, Jan. 2024, doi: 10.1109/TITS.2022.3145363.

[3] S. Hamid et al., "Hybrid Beamforming in Massive MIMO for Next-Generation Communication Technology," Sensors, vol. 23, no. 16, 2023, doi: 10.3390/s23167294.

[4] Z. Wan, Z. Gao, B. Shim, K. Yang, G. Mao, and M. S. Alouini, "Compressive Sensing Based Channel Estimation for Millimeter-Wave Full-Dimensional MIMO with Lens-Array," IEEE Transactions on Vehicular Technology, vol. 69, no. 2, pp. 2337–2342, Feb. 2020, doi: 10.1109/TVT.2019.2962242.

[5] Q. Wan, J. Fang, H. Duan, Z. Chen, and H. Li, "Generalized Bussgang LMMSE Channel Estimation for One-Bit Massive MIMO Systems," IEEE Transactions on Wireless Communications, vol. 19, no. 6, pp. 4234–4246, Jun. 2020, doi: 10.1109/TWC.2020.2981599.

[6] I. Osama, M. Rihan, M. Elhefnawy, S. Eldolil, and H. A. E. A. Malhat, "A Review on Precoding Techniques for mm-Wave Massive MIMO Wireless Systems," International Journal of Communication Networks and Information Security, vol. 14, no. 1, 2022, doi: 10.17762/ijcnis.v14i1.5206.

[7] A. Singh and S. Joshi, "A Survey on Hybrid Beamforming in MmWave Massive MIMO System," Journal of scientific research, vol. 65, no. 01, 2021, doi: 10.37398/jsr.2021.650126.

[8] K. Venugopal, A. Alkhateeb, N. Gonzalez Prelcic, and R. W. Heath, "Channel Estimation for Hybrid Architecture-Based Wideband Millimeter Wave Systems," IEEE Journal on Selected Areas in Communications, vol. 35, no. 9, pp. 1996–2009, Sep. 2017, doi: 10.1109/JSAC.2017.2720856.

[9] S. Park and R. W. Heath, "Spatial channel covariance estimation for mmWave hybrid MIMO architecture," 2016 50th Asilomar Conference on Signals, Systems and Computers, Pacific Grove, CA, USA, 2017, pp. 1424–1428. doi: 10.1109/ACSSC.2016.7869611.

[10] Y. Dong, C. Chen, and Y. Jin, "AoAs and AoDs estimation for sparse millimeter wave channels with one-bit ADCs," 2016 8th International Conference on Wireless Communications & Signal Processing (WCSP), Yangzhou, China, 2016, pp. 1–5, doi: 10.1109/WCSP.2016.7752451.

[11] H. Pirzadeh and A. L. Swindlehurst, "Spectral efficiency of mixed-ADC massive MIMO," IEEE Transactions on Signal Processing, vol. 66, no. 13, pp. 3599–3613, Jul. 2018, doi: 10.1109/TSP.2018.2833807.

[12] W. Tan, S. Li, and M. Zhou, "Spectral and energy efficiency for uplink massive MIMO systems with mixed-ADC architecture," Physical Communication, vol. 50, 2022, doi: 10.1016/j.phycom.2021.101516.

[13] J. Lee, G. T. Gil, and Y. H. Lee, "Channel Estimation via Orthogonal Matching Pursuit for Hybrid MIMO Systems in Millimeter Wave Communications," IEEE Transactions on Communications, vol. 64, no. 6, pp. 2370–2386, Jun. 2016, doi: 10.1109/TCOMM.2016.2557791.

[14] L. Weiland, C. Stockle, M. Wurth, T. Weinberger, and W. Utschick, "OMP with grid-less refinement steps for compressive mmwave MIMO channel estimation," 2018 IEEE 10th Sensor Array and Multichannel Signal Processing Workshop (SAM), Sheffield, UK, 2018, pp. 543–547, doi: 10.1109/SAM.2018.8448789.

[15] X. Liu et al., "Efficient Channel Estimator with Angle-Division Multiple Access," IEEE Transactions on Circuits and Systems I: Regular Papers, vol. 66, no. 2, pp. 708–718, Feb. 2019, doi: 10.1109/TCSI.2018.2869783.

[16] H. Kim, G. T. Gil, and Y. H. Lee, "Two-step approach to time-domain channel estimation for wideband millimeter wave systems with hybrid architecture," IEEE Transactions on Communications, vol. 67, no. 7, pp. 5139–5152, Jul. 2019, doi: 10.1109/TCOMM.2019.2906873.

[17] J. Rodriguez-Fernandez, N. Gonzalez-Prelcic, K. Venugopal, and R. W. Heath, "Frequency-Domain Compressive Channel Estimation for Frequency-Selective Hybrid Millimeter Wave MIMO Systems," IEEE Transactions on Wireless Communications, vol. 17, no. 5, pp. 2946–2960, May 2018, doi: 10.1109/TWC.2018.2804943.

[18] C. Hu, L. Dai, T. Mir, Z. Gao, and J. Fang, "Super-resolution channel estimation for mmWave massive MIMO with hybrid precoding," IEEE Transactions on Vehicular Technology, vol. 67, no. 9, pp. 8954–8958, Sep. 2018, doi: 10.1109/TVT.2018.2842724.

[19] T. Wang, C. K. Wen, S. Jin, and G. Y. Li, "Deep Learning-Based CSI Feedback Approach for Time-Varying Massive MIMO Channels," IEEE

Wireless Communications Letters, vol. 8, no. 2, pp. 416–419, Apr. 2019, doi: 10.1109/LWC.2018.2874264.

[20] H. He, C. K. Wen, S. Jin, and G. Y. Li, "Deep Learning-Based Channel Estimation for Beamspace mmWave Massive MIMO Systems," IEEE Wireless Communications Letters, vol. 7, no. 5, pp. 852–855, Oct. 2018, doi: 10.1109/LWC.2018.2832128.

[21] S. Moon, H. Kim, and I. Hwang, "Deep learning-based channel estimation and tracking for millimeter-wave vehicular communications," Journal of Communications and Networks, vol. 22, no. 3, pp. 177–184, Jun. 2020, doi: 10.1109/JCN.2020.000012.

[22] T. Blumensath and M. E. Davies, "In Greedy Pursuit of New Directions: (Nearly) Orthogonal Matching Pursuit by Directional Optimisation," in 2007 15th European Signal Processing Conference, Poznan, Poland, 2007, pp. 340–344.

[23] Y. Azar et al., "28 GHz propagation measurements for outdoor cellular communications using steerable beam antennas in New York city," 2013 IEEE International Conference on Communications (ICC), Budapest, Hungary, 2013, pp. 5143–5147. doi: 10.1109/ICC.2013.6655399.

[24] M. K. Samimi and T. S. Rappaport, "Ultra-wideband statistical channel model for non-line of sight millimeter-wave urban channels," in 2014 IEEE Global Communications Conference, Austin, TX, USA, 2014, pp. 3483–3489, doi: 10.1109/GLOCOM.2014.7037347.

[25] J. Sung, J. Choi, and B. L. Evans, "Narrowband Channel Estimation for Hybrid Beamforming Millimeter Wave Communication Systems with One-bit Quantization," 2018 IEEE International Conference on Acoustics, Speech and Signal Processing (ICASSP), Calgary, AB, 2018, pp. 3914–3918, doi: 10.1109/ICASSP.2018.8462337.